

A bilayered skin substitute developed using eggshell membrane crosslinked gelatin-chitosan cryogel

Rituparna Saha, Shivali Patkar, Drishti Maniar, Mamatha M. Pillai, Prakriti Tayalia*

1. Protocol for MTT Assay

For MTT assay, film or cryogel samples were given a gentle PBS wash and MTT (0.5 mg/ml, 200 μ l) solution was added per well followed by incubation at 37°C for 4 hours. The solution was then discarded and DMSO (300 μ l) was added to each well to dissolve the formazan crystals and kept on an orbital shaker for 10 minutes. 200 μ l of this solution was then transferred to another 96 well-plate and absorbance at 570 nm was measured using a plate reader (Varioskan LUX).

2. Protocol for Phalloidin/DAPI staining

After 24 hours, cell seeded cryogels were fixed in 4% paraformaldehyde for 10 minutes at room temperature. This was followed by permeabilization with 0.1% Triton X-100 for 10 minutes, blocking with 1% BSA for 30 minutes and staining with phalloidin for 1 hour and with DAPI for another 30 minutes. All steps were carried out at room temperature and was followed by three PBS washes of 5 minutes.

Table S1. Nomenclature and compositions of various blends of gelatin and chitosan for optimization of cryogels and films. Different compositions were tested for various physical parameters to choose the best condition.

Sample name	Total polymer concentration [% w/v]	Gelatin:Chitosan
3% 1:1 GC	3%	1:1
3% 1:5 GC		1:5
4% 1:1 GC	4%	1:1
4% 1:5 GC		1:5
5% 1:1 GC	5%	1:1

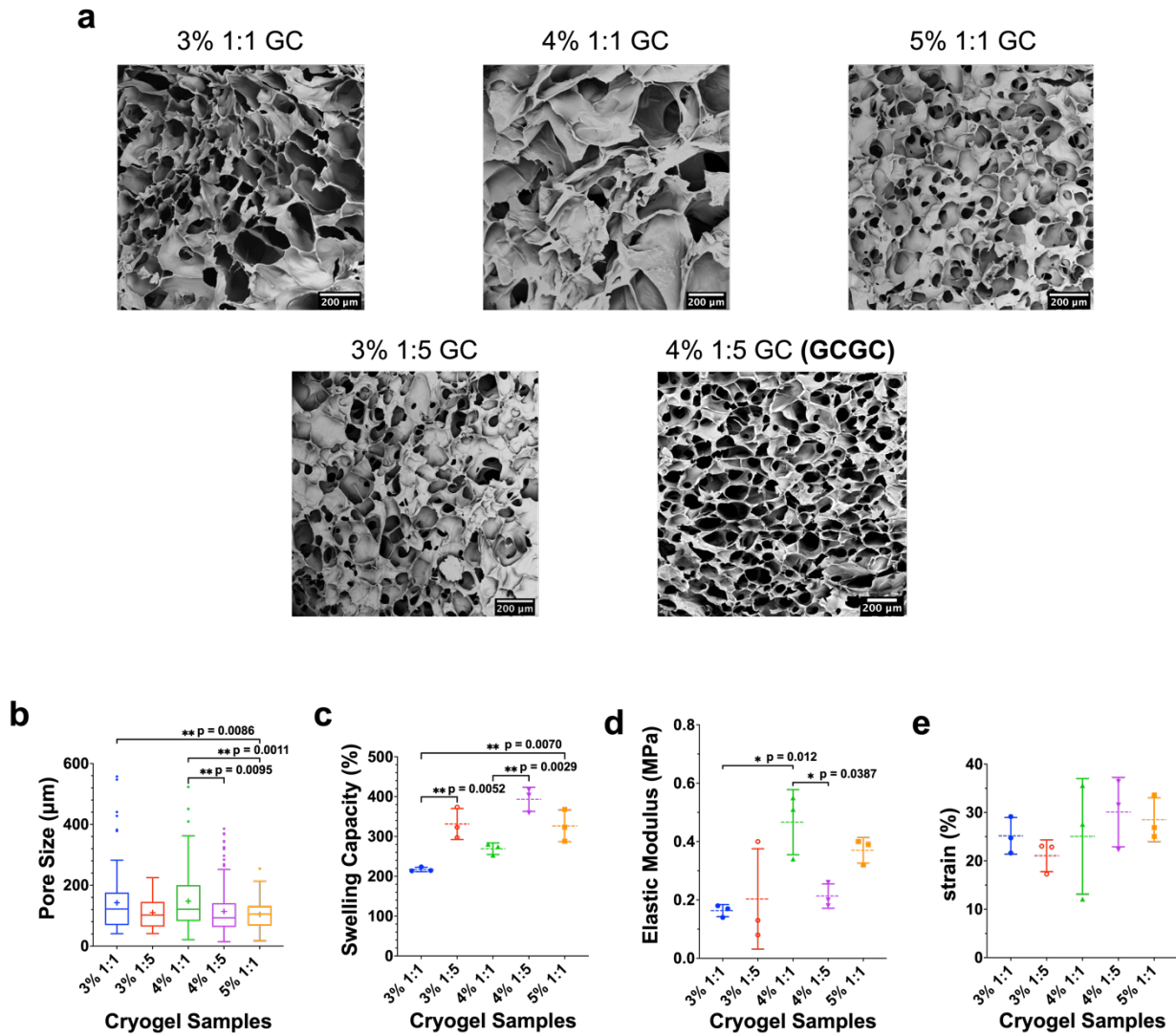


Figure S1. Physical characterization of cryogels for optimization of dermal equivalent. (a) SEM images of cryogels of various compositions of gelatin:chitosan (G:C) depicting their interconnected macroporous structure (scale bar = 200 μ m). (b) Quantification of pore size distribution ($n \geq 100$; whiskers of box plots are plotted by Tukey method), (c) swelling capacity, (d) elastic modulus and (e) % strain at break determined by tensile testing. For graphs c-e, each symbol represents an independent sample. All numerical data are presented as average \pm S.D. and analyzed by one-way ANOVA and Tukey's test.

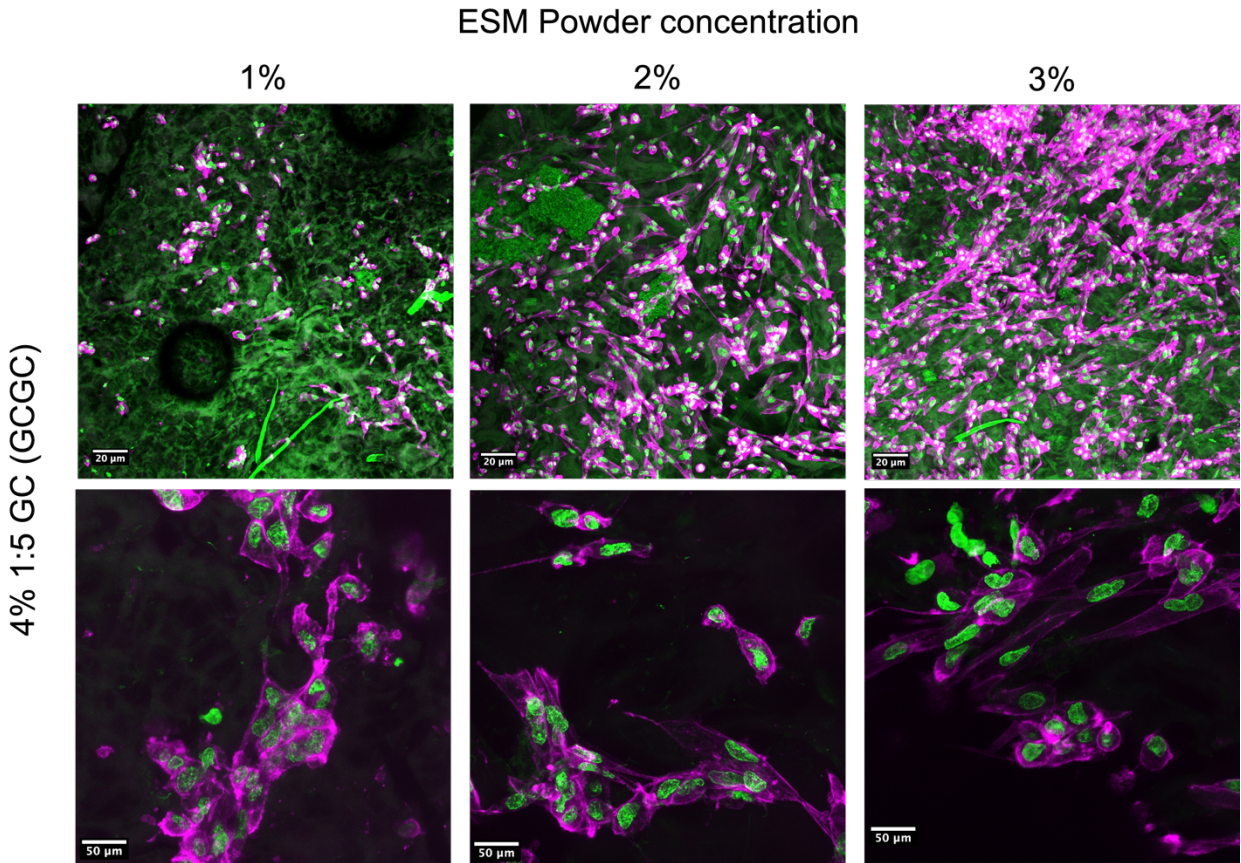


Figure S2. Representative confocal micrographs of Phalloidin (pink) and DAPI (green) stained HADF cells seeded on GCGC (4% 1:5 GC) cryogels incorporated with different concentrations of ESM after 24 hours (scale bar = 20 μm for top panel; 50 μm for bottom panel). Phalloidin represents the actin cytoskeleton of cells while DAPI represents the nuclei of cells. However, autofluorescence of the cryogels in the same emission region as DAPI cause the cryogels (background) to appear green as well. Increasing cell attachment with increase in amount of ESM powder was observed thus, establishing its regenerative potential.

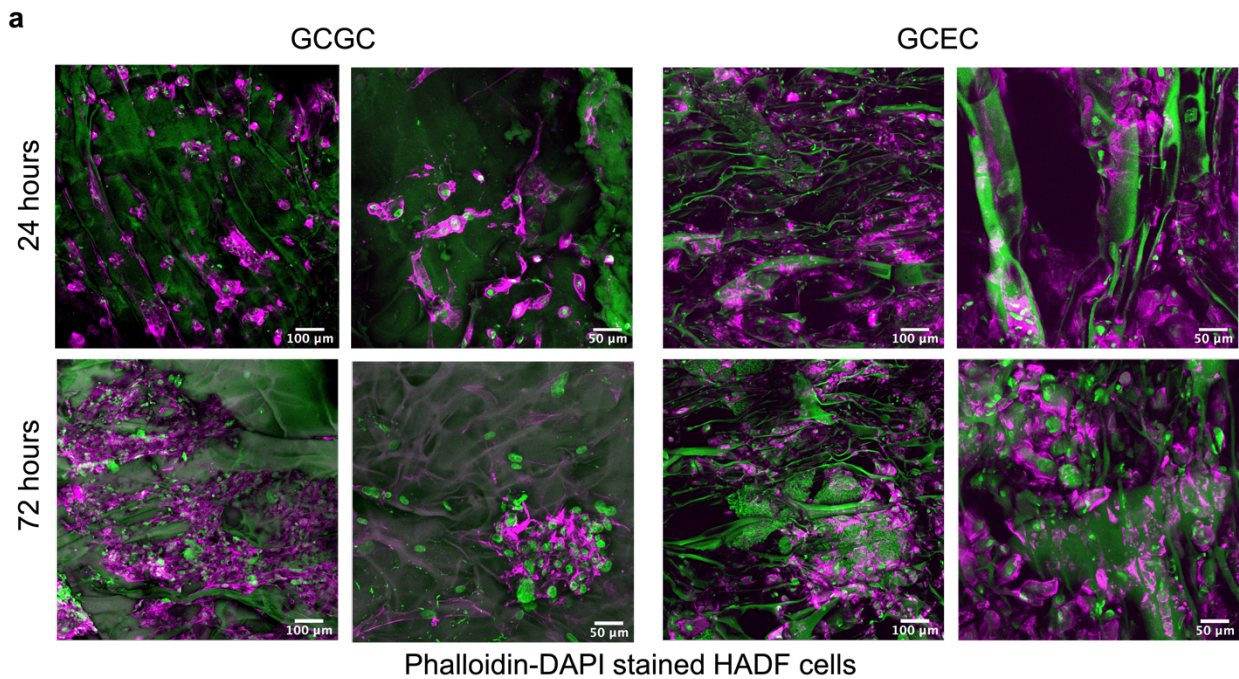


Figure S3. Representative confocal micrographs of Phalloidin (pink) and DAPI (green) stained HADF cells seeded on GCGC and GCEC cryogels at various time intervals. Z-stacks at intervals of 3 μm were captured and merged to create the above maximum intensity projection images.

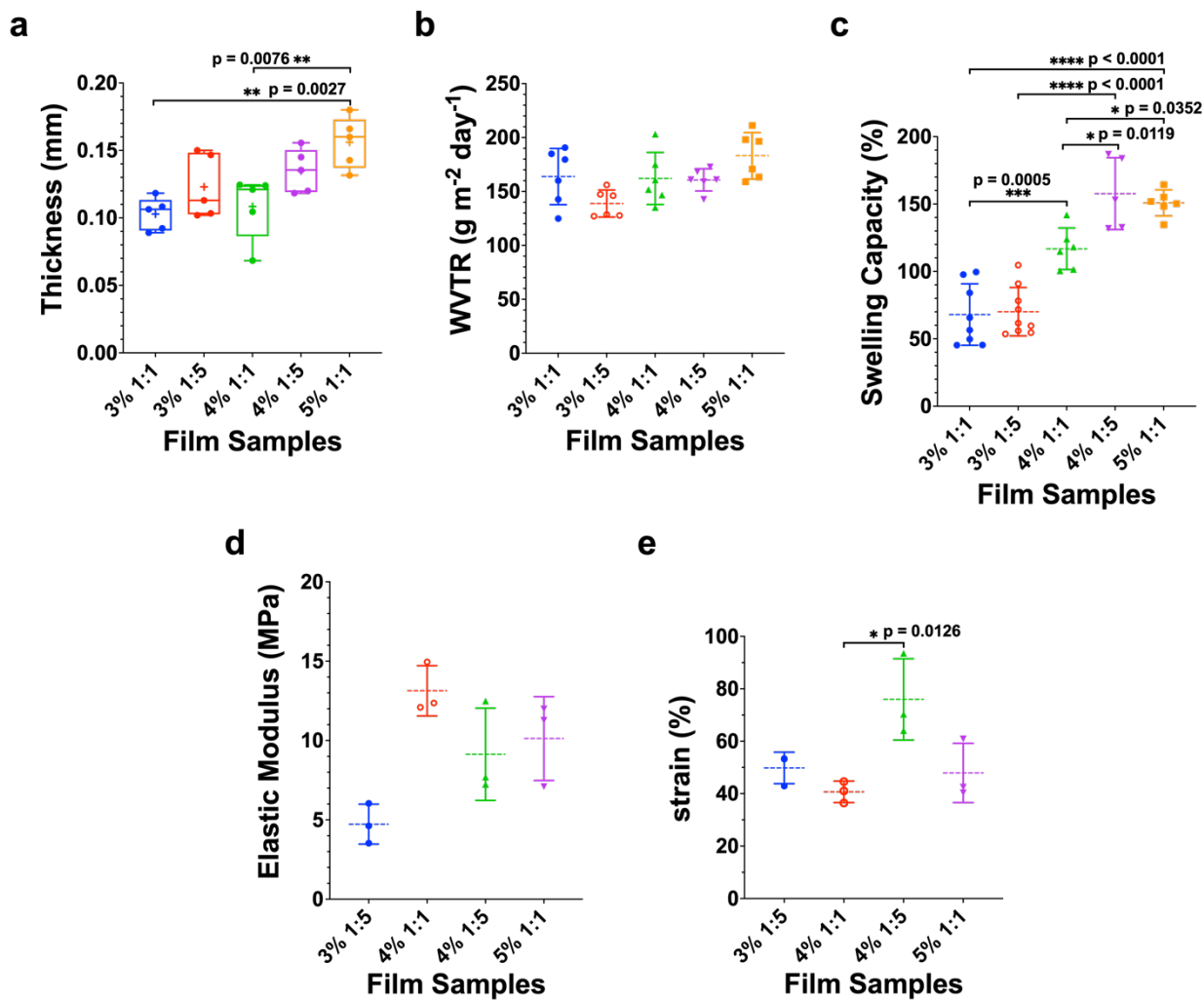


Figure S4. Physical characterization of films for optimization of epidermal equivalent. (a) Quantification of thickness (each symbol represents an average of 10 measurements; whiskers of box plots are plotted by Tukey method). Quantification of (b) water vapor transmission rate (WVTR), (c) swelling capacity, (d) elastic modulus and (e) % strain at break determined by tensile testing. For graphs b-e, each symbol represents an independent sample. All numerical data are presented as average \pm S.D. and analyzed by one-way ANOVA and Tukey's test.

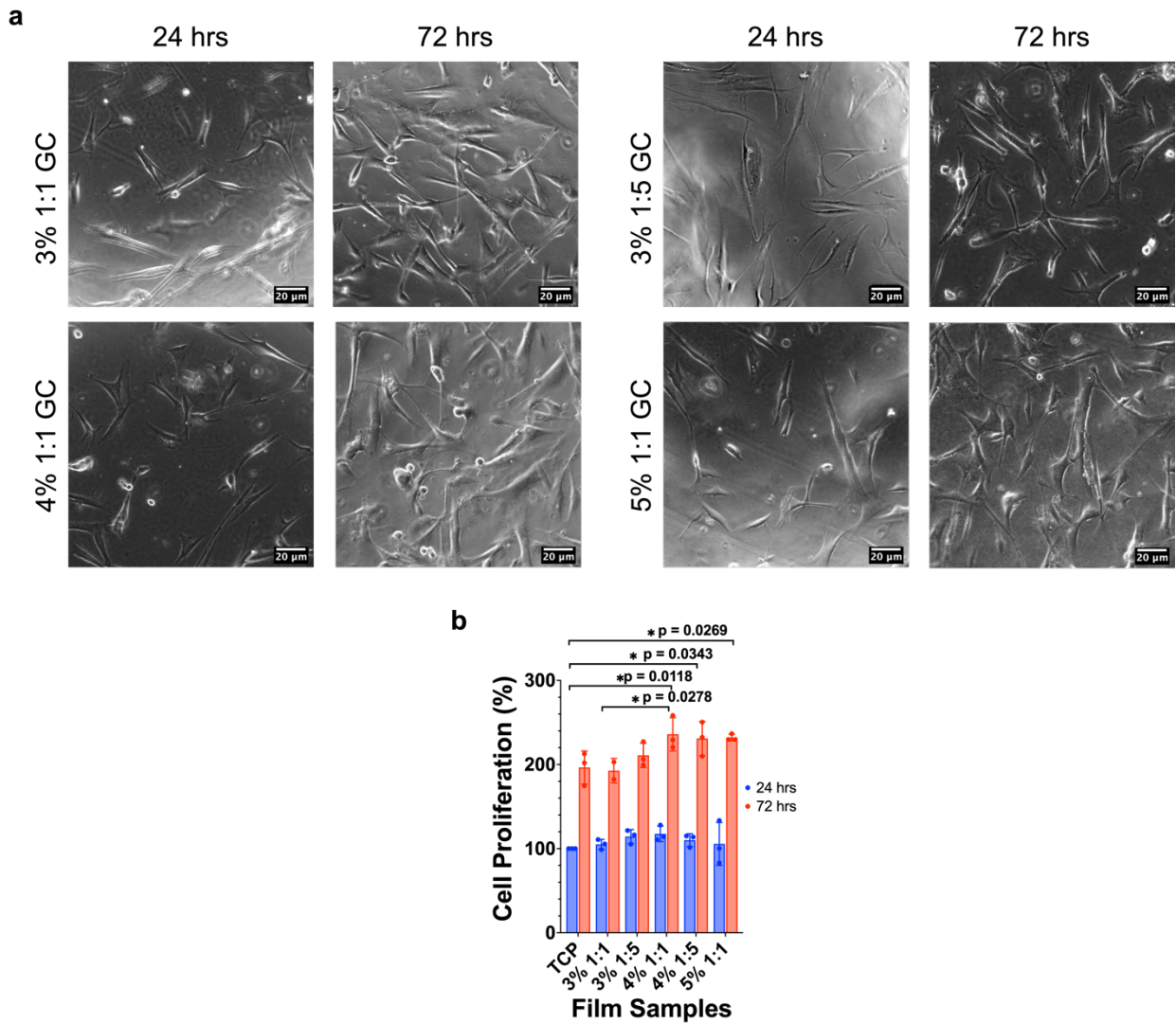


Figure S5. Biological characterization of films for optimization of epidermal equivalent. (a) Phase contrast images of HADF cells grown on films of various compositions of gelatin:chitosan (G:C) for different time intervals (scale bar = 20 μm). (b) Quantification of cell proliferation by MTT assay of HADF cells grown on films for different time intervals (mixed-effect analysis, Tukey's Test). All the film samples were found to be biocompatible and cell growth was comparable to TCP (tissue culture plate).

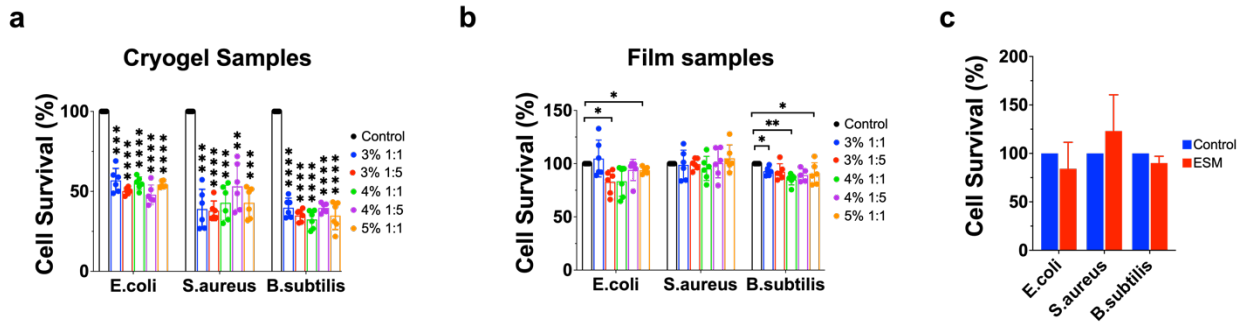


Figure S6. Quantitative analysis of antibacterial efficacy by broth microdilution method. Antibacterial efficacy of (a) cryogels (two-way ANOVA, Dunnett's Test), (b) films (mixed-effect analysis, Dunnett's Test) and (c) ESM ($n = 3$; two-way ANOVA, Tukey's Test. Control represents bacterial culture only. Each symbol represents an independent sample. * $p < 0.05$, ** $p < 0.01$, *** $p < 0.001$, **** $p < 0.0001$. Cryogels showed significant antibacterial activity whereas films lacked such effect possibly due to increased area of interaction between chitosan chains in the cryogels and bacterial cell wall. ESM lacked antibacterial activity.



b

Sample	N [%]	E [%]	L [%]	M [%]
Normal range	13-61%	0-8%	55-86%	0-1%
Scaffold	21	06	72	01
	28	02	69	01
Tegaderm	21	03	75	01
	23	01	75	01

Figure S7. Qualitative and quantitative analysis of dermal irritation test performed on rats. (a) Digital photograph of skin surface when scaffold was removed 7 days after implantation showing no visual signs of allergy or redness. (b) Complete blood count (CBC) analysis of blood collected by retro-orbital bleeding method from 2 rats per group. N = Neutrophil, E = Eosinophil, L = Lymphocyte, M = Monocyte. Counts of various immune cells are within the reference ranges suggesting no inflammatory response generated by the scaffolds.

G	C	GCGC	GCEC	ESM	Bonds
----------	----------	-------------	-------------	------------	--------------

567	565	563	563	565	C=O bending of amide (Amide VI)
687	658	656	663	687	OCN bending of amide (Amide IV)
875	854	853	897	876	C-H bending
1032	1040	1029	1030	1030	C-O and C-O-C stretching of polysaccharides
1080	1090	1085	1076	1067	
1163	1153	1153	1155	1163	
1232		1236	1229	1232	N-H bending with C-N stretching of amide (Amide III)
1383	1379	1383	1380	1382	CH ₂ wag of proline and glycine
1545	1570	1562	1564	1545	N-H bending with C-N stretching of amide (Amide II)
1655	1655	1656	1659	1655	C=O stretching of amide (Amide I), C=N stretching of imine
2878	2880	2880	2878	2878	C-H stretching of alkane
2932	2928	2930	2920	2922	
3443	3389	3422	3431	3427	N-H stretch of primary amine overlapped with O-H stretch of alcohol

Table S2. Characteristic FTIR peaks and their corresponding representative bonds